Abstract Volume
11th Swiss Geoscience Meeting

Lausanne, 15th – 16th November 2013

19. Earth System Science related Earth Observation

sc | nat

Swiss Academy of Sciences
Akademie der Naturwissenschaften
Accademia di scienze naturali
Académie des sciences naturelles

UNIL | Université de Lausanne
Faculté des géosciences
et de l'environnement

19. Earth System Science related Earth Observation

Michael E. Schaepman, Brigitte Buchmann, Alain Geiger

Swiss Commission for Remote Sensing,
Swiss Geodetic Commission

TALKS:

19.1 Garonna I., De Jong R., De Wit A., Mücher C.A., Schmid B., Schaepman, M.E.: Testing Land Surface Phenology (LSP) indicators in Europe

19.2 Matasci G., Volpi M., Kanevski M., Tuia D.: Hyperspectral and LiDAR data fusion for high resolution urban land cover/land use classification

19.3 Salvini D., Parada I., Jerik A. C.: Defining the geodetic datum for a tectonically active country

19.4 Schanz A., Studer S., Hocke K., Kämpfer N.: The Diurnal Cycle in Stratospheric Ozone: Observation, Simulation and Understanding

19.5 Torabzadeh H., Morsdorf F., Leiterer R., Schaepman M.: Determining forest species composition using imaging spectrometry and airborne laser scanner data

19.6 Zwieback S., Hajnsek I.: Soil Moisture Effects in Differential SAR Interferometry – Impact on estimated deformations and elevations

POSTERS:

P 19.1 Parkan M., Tuia D.: Modelling coastal atmospheric temperature in Greenland with support vector regression

P 19.2 Volpi M., Matasci G., Kanevski M., Tuia D.: Interactive multisensor change detection in remote sensing images via kernel canonical correlation transformation

19.1

Testing Land Surface Phenology (LSP) indicators in Europe

Garonna I.[1], De Jong R.[1], De Wit A.[2], Mücher C.A. [2], Schmid B.[3] & Schaepman, M.E.[1]

[1] *Remote Sensing Laboratories (RSL), Department of Geography, University of Zurich, Winterthurerstr. 190, 8057 Zurich, Switzerland*
[2] *Team Earth Observation and Environmental Informatics, Alterra, Wageningen University and Research Centre, P.O. Box 47, NL-6700 AA Wageningen, the Netherlands*
[3] *Institute of Evolutionary Biology and Environmental Studies, University of Zurich, Winterthurerstr. 190, 8057 Zurich, Switzerland*

Significant recent increases in vegetation activity over time (i.e. *greening)* have been identified over Europe (e.g. *Stöckli and Vidale*, 2004), and associated both with climatic changes and with large-scale human interventions, including land-use change (*de Jong et al.*, 2013). The long-standing human managing and shaping of the landscape make the European region a particularly challenging – and interesting – region of study for environmental change studies.

Land Surface Phenology (LSP) focuses on intra-annual dynamics of vegetation activity as observed from satellite observations. As such, this field plays a key role in understanding the terrestrial carbon budget, as well as the response of terrestrial ecosystems to environmental change.

In this study, we characterize LSP changes in Europe's eco-regions for the last 30 years. We use the latest version of the 8-km Global Inventory Modeling and Mapping Studies (GIMMS) Normalized Difference Vegetation Index dataset (third generation, or NDVI-3g) to retrieve LSP metrics for Pan-Europe for the last three decades (1982–2011). Each year of NDVI data is processed using the Harmonic Analysis of Time Series (HANTS) algorithm, producing smooth NDVI annual profiles on a pixel-by-pixel basis. We derive LSP metrics for each year, namely Start, End and Length of Growing Season, by applying the $\text{Midpoint}_{\text{pixel}}$ local threshold method, based on the White et al. (2009) inter-comparison.

A landscape-based stratification, using the European Landscape Classification (LANMAP) (*Mücher et al.*, 2010) allows us to examine LSP characteristics and trends for the different European eco-regions. We demonstrate statistically significant shifts in LSP metrics over the study period, with a general lengthening of the growing season in Europe of approximately 0.3 days year^{-1}. LSP trends varied significantly between eco-regions, and we discuss potential reasons for these spatially diverse trends.

REFERENCES

de Jong, R., et al. (2013), Spatial relationship between climatologies and changes in global vegetation activity, Global Change Biology, 19(6), 1953-1964.

Mücher, C. A., J. A. Klijn, D. M. Wascher, and J. H. J. Schaminée (2010), A new European Landscape Classification (LANMAP): A transparent, flexible and user-oriented methodology to distinguish landscapes, Ecological Indicators, 10(1), 87-103.

Stöckli, R., and P. L. Vidale (2004), European plant phenology and climate as seen in a 20-year AVHRR land-surface parameter dataset, International Journal of Remote Sensing, 25(17), 3303-3330.

White, M. A., et al. (2009), Intercomparison, interpretation, and assessment of spring phenology in North America estimated from remote sensing for 1982–2006, Global Change Biology, 15(10), 2335-2359.

19.2

Hyperspectral and LiDAR data fusion for high resolution urban land cover/land use classification

Matasci Giona[1], Volpi Michele[1], Kanevski Mikhail[1] & Tuia Devis[2]

[1] *Center for Research on Terrestrial Environment (CRET), University of Lausanne, Quartier UNIL-Mouline, CH-1015 Lausanne. (giona.matasci@unil.ch)*
[2] *Laboratory of Geographic Information Systems (LaSIG), Ecole Polytechnique Fédérale de Lausanne, EPFL Station 18, CH-1015 Lausanne.*

In this study we investigated the possible synergies between hyperspectral and LiDAR-derived data for the detailed thematic classification of the land cover/land use in an urban environment (Dalponte et al. 2008; Priestnall et al. 2000). To this end, we could resort to two datasets available for the 2013 IEEE GRSS Data Fusion Contest describing a neighbourhood of the city of Houston, USA. The datasets consisted of a hyperspectral image with 144 VNIR spectral bands and a Digital Surface Model extracted from a LiDAR acquisition. The two layers were co-registered and presented a spatial resolution of 2.5 meters. The purpose was to discriminate 15 highly overlapping classes of interest related to the land cover/land use present in the considered urban scene.

First, we processed the remotely sensed image with a histogram matching procedure with the aim of removing the shadows cast by the clouds. Then, we extracted spatial features (morphological opening and closing filters and the associated top hat operators) at various scales both from the hyperspectral image (after PCA transformation) and from the raw LiDAR height map (Tuia et al. 2009; Benediktsson et al. 2003). Additionally, the set of features has been complemented with spectral indices, namely with variations of the NDVI based on different band combinations.

Subsequently, after having stacked all the extracted features into a single dataset, a Support Vector Machine classifier has been trained using the available labeled samples. A prediction over the entire extent of the image has been performed to obtain the final classification map. After a suitable post-processing involving a spatial majority vote filtering with a moving window, the resulting thematic map accurately delineates the various land cover/land use classes in the scene.

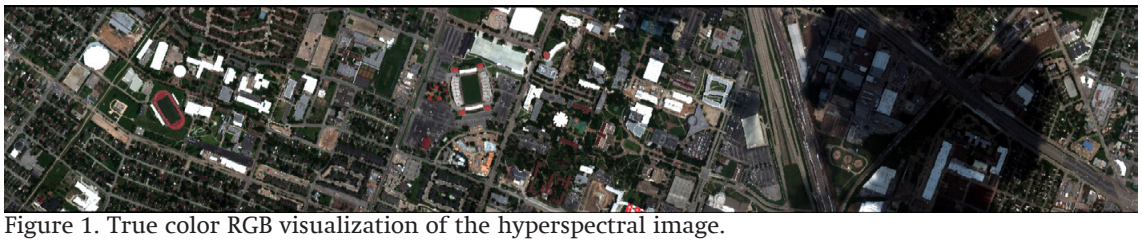

Figure 1. True color RGB visualization of the hyperspectral image.

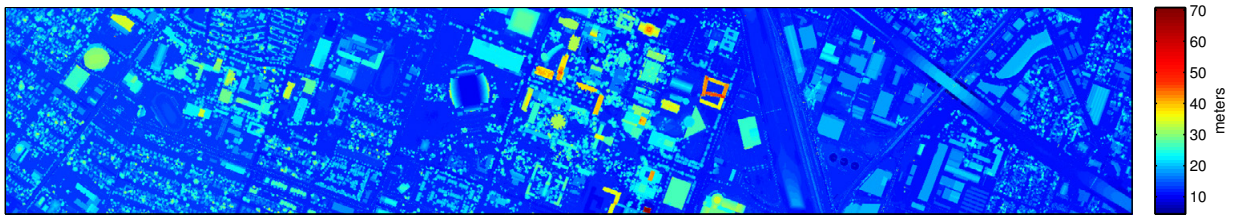

Figure 2. Digital Surface Model derived from the LiDAR acquisition.

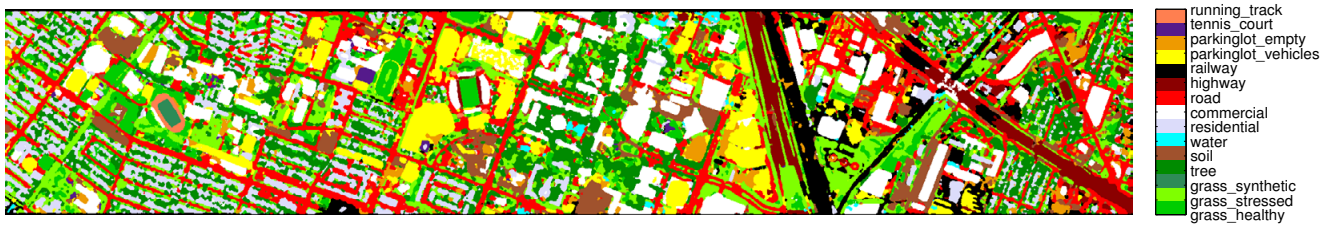

Figure 3. Final classification map with 15 classes (Kappa statistic = 0.945).

REFERENCES

Benediktsson, J. A., Pesaresi, M., & Amason, K. 2003. Classification and feature extraction for remote sensing images from urban areas based on morphological transformations. IEEE Transactions on Geoscience and Remote Sensing, 41(9), 1940-1949.

Dalponte, M., Bruzzone, L., & Gianelle, D. 2008. Fusion of hyperspectral and LIDAR remote sensing data for classification of complex forest areas. IEEE Transactions on Geoscience and Remote Sensing, 46(5), 1416-1427.

IEEE GRSS Data Fusion Contest 2013, Online: http://www.grss-ieee.org/community/technical-committees/data-fusion/

Priestnall, G., Jaafar, J., & Duncan, A. 2000. Extracting urban features from LiDAR digital surface models. Computers, Environment and Urban Systems, 24(2), 65-78.

Tuia, D., Pacifici, F., Kanevski, M., & Emery, W. J. 2009. Classification of very high spatial resolution imagery using mathematical morphology and support vector machines. IEEE Transactions on Geoscience and Remote Sensing, 47(11), 3866-3879.

19.3

Defining the geodetic datum for a tectonically active country

Salvini Dante[1], Parada Ivan[2], Jerik Axpuak Calderas[3]

[1]*BSF Swissphoto AG, Dorfstrasse 53, CH-8105 Regensdorf-Watt (dante.salvini@bsf-swissphoto.com)*
[2]*Instituto Geográfico Nacional, Avenida Las Américas 5-76, zona 13, GT-01013 Guatemala-City (ivan.parada@ign.gob.gt)*
[3]*Registro de Información Catastral, 21 calle 10-58, zona 13, GT-01013, Guatemala-City (jaxpuac@ric.gob.gt)*

Guatemala is located between the Pacific Ocean and the Caribbean Sea at a latitude of 15° N. From a geological point of view, the country lies within an area of active plate convergence and transversal plate motion. The Motagua Fault, part of the boundary between the Caribbean and North American tectonic plates, transects Guatemala. In addition, the Middle America Trench is located along the southwest coast. Here, the Cocos Plate subducts beneath the Caribbean Plate. Due to this configuration, earthquakes occur frequently, many of them killing people and causing damages. The last major earthquake occurred in November 2012 near the Pacific coast and caused irreversible displacements of the ground in the order of several centimeters. The quantification of these displacements and the extension of the affected area were only possible because the country runs a continuously operating reference network (CORS). The network consists of 17 GNSS stations distributed over the entire country and was realized with funding and support of Switzerland (SECO, mixed credit project in Guatemala). The periodical computation of the coordinates of each station allows tracking of the displacements. In other words, the CORS acts as a monitoring system of the earth surface. The results over the last 12 years of the 3 longest-running stations show a continuous movement of the tectonic plates mentioned before (see fig. 1). In addition to the continuous movement, it is well known that earthquakes can produce abrupt shifts.

The primary scope of the installation and the operation of the CORS is to support surveying operations, notably land surveying and the cadastral land register. It is considered state of the art that countries base their local reference systems on CORS networks. Such a local reference system includes the official national coordinate and height systems with all their basic definitions (reference ellipsoid, geoid model and map projection). All surveying activities are then based on that one national reference system. When defining national reference systems, it is normally assumed that the country is geologically stable or at least that the displacement of the plate on which the country lies is homogeneous. These prerequisites are not given for Guatemala. This fact forces the surveyors to take into account the geological displacements when defining the reference system. In 2012, as the full CORS of Guatemala was brought into service, the Swiss consultants proposed a unique approach for a reference system, consisting of two phases. In a first step, the coordinates of the 17 sites have to be defined according to the global reference frame (ITRF). These coordinates can be obtained by international computing centers, in the case of Guatemala by SIRGAS (Geocentric Reference System for the Americas). These coordinates constitute the basis for every surveying activity. For a period of approx. 8 years, the coordinates of the sites maintain their validity regardless of the moving plates (estimated displacement in this time is 10 cm). After three to four years, the continuous computation of the station coordinates done by SIRGAS allows the derivation of a velocity model which approximates the movement of the plates. During the subsequent years, the model has to be kept up to date (e.g. including shifts due to earthquakes) and validated. Based on the discrete velocity model, a grid (so called NTv2) covering the entire country can be derived. In the second and final phase, this grid is used to switch between the current epoch in which surveying is done and the epoch in which the reference system was defined. This transformation is needed to keep every position (coordinate) regardless of its time of measurement in a unique and consistent reference frame.

The National Geographic Institute of Guatemala is now refining the Swiss proposal in order to implement the new reference system as soon as possible.

REFERENCES

Salvini D, Brockmann E. 2013, Marco de referencia y proyección para Guatemala, BSF Swissphoto 2013
Brockmann E. 2009: Coordinate Reference Frame Definition Guatemala, swisstopo 2009.
Sanchez L., Cruz O. 2012, SIRGAS and the earthquake of November 7th 2012 in Guatemala, SIRGAS 2012.
Department of Geological an Environmental Sciences 2005, Field Guide to Guatemala Geology, Stanford University 2005
http://www.swisstopo.ch, last visit 31.08.2013
http://en.wikipedia.org, last visit 31.08.2013
http://www.sirgas.org, last visit 31.08.2013

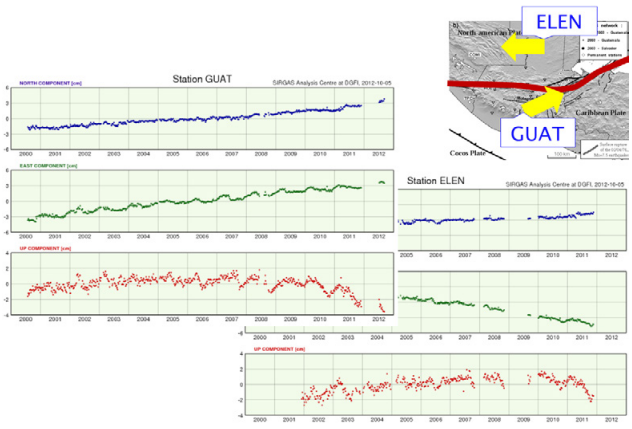

Figure 1.Plots of the continuous displacements monitored for the site GUAT (Carribean plate) and ELEN (North American plate)

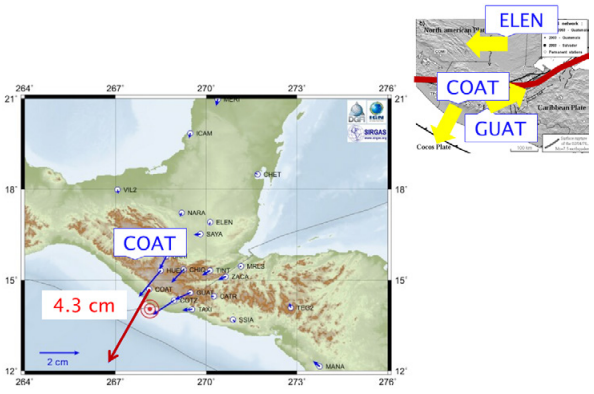

Figure 2. Earthquake of Nov. 2012 caused a displacement of 4.3 cm at the site COAT (near the Middle America Trench)

19.4

The Diurnal Cycle in Stratospheric Ozone: Observation, Simulation and Understanding

Schanz Ansgar, Studer Simone, Hocke Klemens, Kämpfer Niklaus

Institute of Applied Physics and Oeschger Centre for Climate Change Research, University of Bern, Sidlerstr. 5, CH-3012 Bern (ansgar.schanz@iap.unibe.ch)

The diurnal cycle in stratospheric ozone only amounts a few percent. This small amplitude significantly affects trend estimates of the stratospheric ozone layer. The ozone layer is expected to recover by about +1% per decade until 2050. Since satellite orbits differ or slightly drift in local solar time, the diurnal cycle in stratospheric ozone will bias global ozone data sets from satellites.

For correction of the diurnal bias we have to observe, to simulate and to understand the diurnal cycle in stratospheric ozone at each geographic location. Seasonal and interannual variations of the diurnal ozone cycle also should be taken into account (Figure 1).

We present a climatology of the diurnal ozone cycle derived from 17 years of ozone microwave radiometry at University of Bern (Figure 2). We discuss the intercomparison between the observations and simulation results of the Whole Atmosphere Community Climate Model (WACCM). The simulation helps us to understand the chemical, radiative, dynamical and thermal forcings which are responsible for the diurnal cycle in stratospheric ozone.

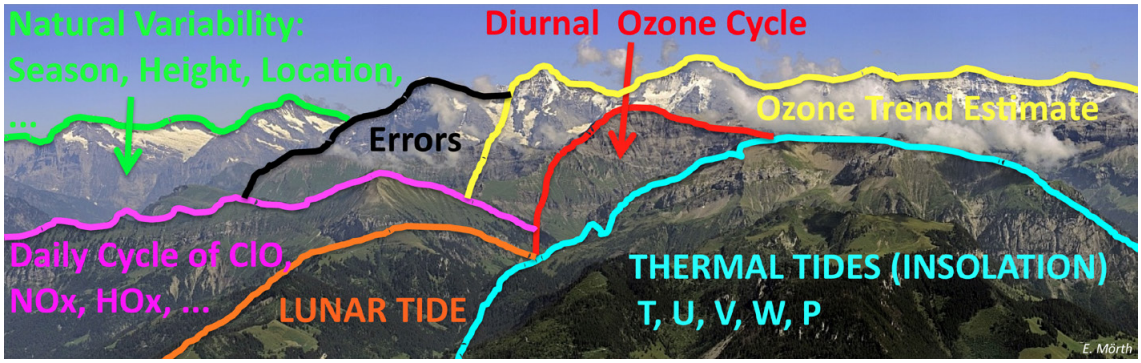

Figure 1. Illustration of the versatility of the diurnal cycle in stratospheric ozone which depends on many other factors such as systematic instrument errors, thermal tides and diurnal variations in ozone depleting substances. The diurnal ozone cycle can be utilized as a benchmark for the accuracy of ozone measurement and retrieval techniques. A good knowledge of the diurnal ozone cycle is needed for the correction of diurnal biases in ozone data sets from satellites.

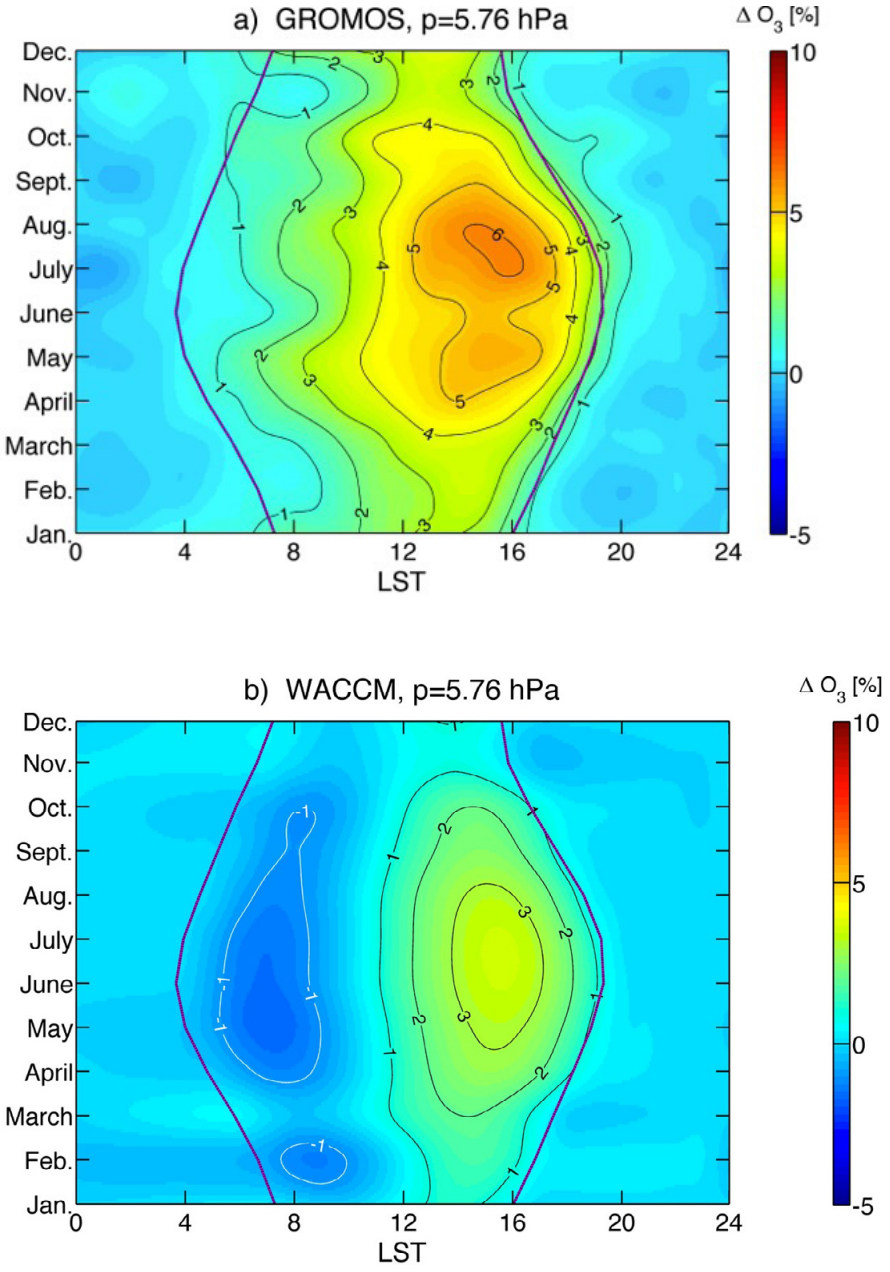

Figure 2. Climatology of the diurnal ozone variation at about 35 km altitude: a) derived from 17 years of ozone observations at Bern, b) simulated by the chemistry-climate model WACCM. The relative ozone variation with respect to midnight ozone is maximal in the afternoon during summer. The two black curves denote the Local Solar Time (LST) of a solar zenith angle of 90 deg. (Studer et al., 2013)

REFERENCES

Studer S., K. Hocke, A. Schanz, H. Schmidt, N. Kämpfer: A climatology of the diurnal variation of stratospheric and mesospheric ozone over Bern, Switzerland, submitted to Atmos. Chem. Phys. Discuss., July 2013

19.5

Determining forest species composition using imaging spectrometry and airborne laser scanner data

Torabzadeh Hossein, Morsdorf Felix, Leiterer Reik, Schaepman E. Michael

Remote Sensing Laboratories, Department of Geography, University of Zurich, Winterthurerstrasse 190, 8057 Zurich, Switzerland, Email: hossein.torabzadeh@geo.uzh.ch

Forests cover almost one third of the total land surface of the Earth and play an important role in the global energy- and matter fluxes between atmosphere and the land surface. Assessing and quantifying forest ecosystem goods and services (associated with water refinement, carbon sequestration, biodiversity, or wildlife habitats) and their underlying processes helps to develop sustainable management strategies and to project biogeochemical cycles under changing climate conditions (Fisher et al., 2009) . Particularly the tree species composition is an important aspect of forest monitoring as well as for management planning. Assessing of tree species composition with traditional fieldwork is labor-intensive, time-consuming and mostly limited by spatial extent; accordingly, remote sensing data enables to overcome these limitations.

Although different tree species often have unique spectral signatures, mapping based on spectral reflectance properties alone is often an ill-posed problem, since the spectral signature is as well influenced by age, canopy gaps, shadows and background characteristics. Thus, reducing the unknown variation by knowing the structural parameters of different species (e.g. branching and foliage distribution) should improve determination procedures (Holmgren & Persson, 2004).

In this study we combine imaging spectrometry (IS) and airborne laser scanning (ALS) data in a broadleaf dominated forest in the Swiss Jura (latitude 47°28'N, longitude 8°21'E) to differentiate tree species more accurately as single-instrument data could do. Spectral information has been acquired by Airborne imaging spectrometry Prism Experiment (APEX) in 285 bands (400 - 2500 nm). A small footprint, full-waveform RIEGL light detection and ranging (LiDAR) system has been deployed to scan the study area under leaf-on conditions. To validate the results, tree location and species, crown dimensions, diameter in breast height (DBH) and understory condition were derived using a field map system. ALS and IS datasets was scrupulously co-registered so that miss-alignment differences remained less than half size of the IS data pixel size (approximately ±1 m). Minimum noise fractions were calculated from IS data, while, within each image pixel, structurally related statistics along the vertical (e.g. height percentiles) were derived from the full-waveform ALS data. Additionally, the full-waveform information (e.g. echo width and amplitude) was statistically evaluated for each pixel and at different heights.

Due to high dimensionality of multiple sources data that we have, support vector machine (SVM) classifier has been deployed for distinguishing the eight most prevalent tree species in our study area. The spatially explicit information layers containing both, the spectral and structural components from the IS and ALS datasets, were then combined together in the pixel-based image classification procedure.

The final map, improved on single system products, provides the distribution and fraction of each tree species throughout our forest site. A thorough accuracy analysis for each species reveals which species profit most from which variables from the exhaustive structural and/or spectral feature set for its discrimination. We conclude, that the combined use of multi-source ALS and IS data significantly improves the overall accuracy of the tree species classification but is still limited in dense forest areas with deciduous trees, where the individual crowns merged into each other and prevent an unambiguous assignment of a specific tree species.

REFERENCES

Fisher, Brendan, R. Kerry Turner & Paul Morling. Defining and Classifying Ecosystem Services for Decision Making. Ecological Economics 68.3 (2009): 643-53.

Holmgren, Johan & Asa Persson. Identifying Species of Individual Trees Using Airborne Laser Scanner.Remote Sensing of Environment 90.4 (2004): 415-23

19.6

Soil Moisture Effects in Differential SAR Interferometry – Impact on estimated deformations and elevations

Zwieback Simon[1] & Hajnsek Irena [1,2]

[1]*Institute of Environmental Engineering, ETH Zurich, Schafmattstr. 6, CH-8093 Zurich (zwieback@ifu.baug.ethz.ch)*
[2]*Microwaves and Radar Institute, German Aerospace Center, PO BOX 1116, D-82234 Wessling*

Repeat-pass Synthetic Aperture Radar (SAR) Interferometry (or Differential SAR Interferometry, DInSAR) is a valuable remote sensing technique as it is sensitive to deformations or the height of scatterering objects (Gabriel et al. 1989). Due to the first sensitivity, it is a common tool for studying subsidence phenomena (e.g. due to groundwater extraction or soil freezing/thawing) or mass movements; due to the second, it allows for the estimation of digital surface models or maps of vegetation height.

This is done by combining two SAR images acquired at different times: during this time interval, the soil moisture (SM) content can change and this change is hypothesized to influence the phase Φ, from which deformations or height are inferred. If this influence is indeed present, these retrieved deformations or heights will be erroneous.

Such an effect was first postulated 25 years ago by Gabriel et al. (1989) – since then a handful of dedicated experiments and observational studies have yielded inconclusive (and partially inconsistent) results (Rudant et al. 1996; Morrison et al. 2011). Thus the prevalence, sign and size of these influences remain poorly understood.

We propose to statistically analyze the observed phase (two L-band airborne campaigns) as a function of SM changes (measured in situ) using regression techniques; this allows us to i) determine whether these effects are significant; ii) estimate their size; iii)compare this to predictions of proposed models/ explanations; and iv) gauge their impact on retrieving deformations or heights.

The results reveal that soil moisture changes influence the observed phase in both campaigns. Optional figures 1 and 2 show the linear dependence of Φ on SM changes: this slope term β is predominantly positive and significant. This pattern is consistent for both campaigns; there are, however, large inter- and intra-field variations present. The positive sign corresponds to a movement of the soil away from the antenna as the soil becomes moist.

The size of the linear slope term β is usually on the order of 5, but much larger sensitivities occur for certain fields in the CanEx campaign. For illustration: a slope of 5 corresponds to the following: if soil moisture changes by 10%, the phase changes by around 30°.

This size of the slope term as well as its sign can be compared to the predictions of possible origins of the soil moisture effect. Three such explanations have been advanced:

1. Penetration depth hypothesis: the phase is related to the absorption in the soil (Nolan 2003). The predicted sign is opposite to the observed one.
2. Clay swelling: certain soils swell as they become moist, corresponding to a movement towards the sensor and a negative (i.e. opposite to the observed) sign of the effect.
3. Dielectric volume scattering: inhomogeneities within the soil lead to scattering, their apparent distance (optical path) increases as the soil becomes wet (Rudant et al. 1996; de Zan et al. 2013). The sign and also the magnitude (which depends on the specific parameterizations) are compatible with the observations.

These results show that for the data sets studied these effects are significant and only consistent with volume scattering, but not with the other two explanations. This insight can prove beneficial for understanding and also predicting the impact of soil moisture changes, leading to the possibility to estimate soil moisture or provide corrections for the chief applications of the technique: deformation and elevation measurements. The latter would be necessary if these effects were larger than the random noise, and indeed this is the case in the present data sets. In these campaigns, soil moisture induced phases of 90° (and larger) have been observed: this corresponds to a deformation of 3 cm and is much larger than the noise and than typically studied subsidence phenomena conidering the time scale of several days. Similar conclusions also apply to the estimation of elevations, where preprocessing assures that the random noise in the phase is much smaller than 90°. These influences thus have to be taken into consideration for a reliable estimation of deformations using DInSAR, e.g. for monitoring groundwater-related subsidence or tectonic movements.

REFERENCES

de Zan, F., Parizzi, A., Prats-Iraola, P. & Lopez-Dekker, P. 2013: A SAR Interferometric Model for Soil Moisture. IEEE Trans. Geosci. Remote Sens., in press.

Gabriel, A., Goldstein, R. & Zebker, H. 1989: Mapping small elevation changes over large areas: Differential radar interferometry. J. Geophys. Res. 94, 9183-9191.

Morrison, K., Bennett, J., Nolan, M. & Menon, R. 2011: Laboratory Measurement of the DInSAR Response to Spatiotemporal Variations in Soil Moisture. IEEE Trans. Geosci. Remote Sens. 49, 3815-3823.

Nolan, M. 2003: Penetration depth as a DInSAR observable and proxy for soil moisture. IEEE Trans. Geosci. Remote Sens. 41, 532-537.

Rudant, J., Bedidi, A., Calonne, R., Massonnet, D., Nesti, G. & Tarchi, D. 1996: Laboratory Experiment for the Interpretation of Phase Shift in SAR Interferograms. Proceedings of FRINGE.

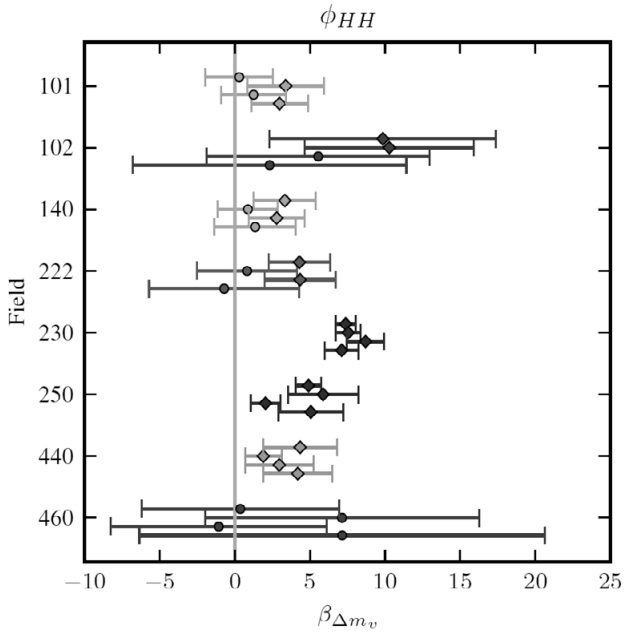

Fig. 1: Estimated linear dependence β of the HH phase on soil moisture for the AGRISAR campaign: the coefficients for each of the four samples within the fields are given by the markers, the error bars denote the 95% confidence intervals.

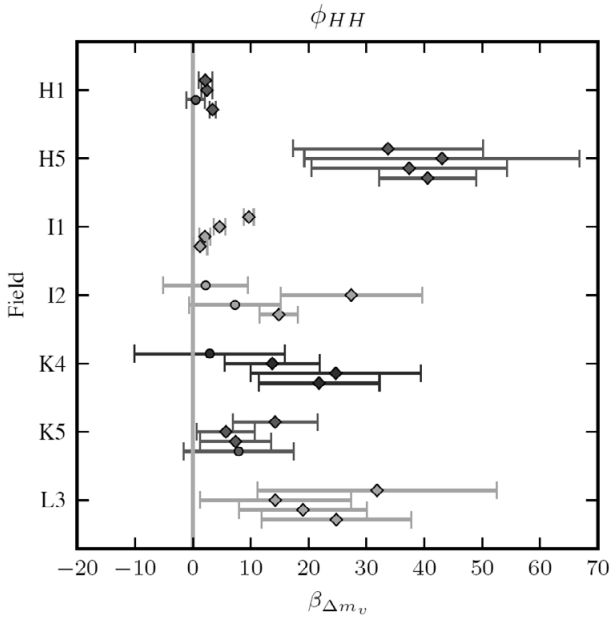

Fig. 2: Same as Fig. 1 but for the CanEx campaign.

P 19.1

Modelling coastal atmospheric temperature in Greenland with support vector regression

Matthew Parkan[1], Devis Tuia[1]

[1]*Laboratoire des Systèmes d'Information Géographique, Ecole Polytechnique Fédérale de Lausanne, Switzerland.*
{matthew.parkan,devis.tuia}@epfl.ch

In the recent years, global climate change has induced thinning of the Greenland ice sheet and an evergrowing loss of sea ice in the Arctic (Abdalati et al, 2001, Krabill et al., 2004). Various local and regional forcing mechanisms and feedback interactions between offshore and inshore variables in coastal areas are currently under scrutiny, but are not yet well understood. One of the key variables influencing the rate of ice disappearance is atmospheric temperature (Tedesco, 2007, Tedesco and Miller, 2007). In this paper, we present a statistically derived model that links coastal atmospheric temperature to offshore conditions, such as expanding open water areas (Rennermalm et al., 2009), sea level pressure or wind speed (Kobashi et al, 2011) at six weather stations on the Coast of Greenland. Our aim is to observe statistical relationships between variations in atmospheric temperatures and changes in offshore conditions. To study these relations, a machine learning approach based on a nonlinear model, support vector regression (SVR, Schölkopf and Smola, 2002), is considered.

Based on a combination of daily in situ (i.e., wind velocity, sea level pressure, cloud ceiling height) and remotely sensed (i.e. sea surface temperature, sea ice concentration) data, a series of daily predicting features are constructed for the years 1981-2012. Daily temperature averages are considered as dependent variables. Two experiments are conducted:

In the first experiment, temperatures predictions by the SVR are compared to a widely used linear model, a multivariate linear regression (LR) with the same independent variables. Results of the SVR indicate that prediction NRMSE of 10–15% are routinely achievable, which are between 2% and 4% lower than when using the linear model.

In the second experiment, individual models are built for each month of the year. Prediction errors are found to be smaller in summer months and/or at lower latitudes (Stations Prins Chistian Sund or Aasiaat, 1.5 – 2°C, 9-10% error).

REFERENCES

Abdalati, W. and Steffen, K. 1992: Snowmelt on the Greenland ice sheet as derived from passive microwave satellite data, Journal of Climate, 10, 165–175.

Kobashi, T., Kawamura, K., Severinghaus, J. P., Barnola, J., Nakae- gawa, T., Vinther, B. M., Johnsen, S. J., and E., B. J. 2011: High variability of Greenland surface temperature over the past 4000 years estimated from trapped air in an ice core, Geophysical Research Letters, 38, L21 501.

Krabill, W., Hanna, E., Huybrechts, P., Abdalati, W., Cappelen, J., Csatho, B., Frederick, E., Manizade, S., Martin, C., Sonntag, J., et al. 2004: Greenland ice sheet: increased coastal thinning, Geophysical Research Letters, 31.

Rennermalm, A. K., Smith, L. C., Stroeve, J. C., and Chu, V. W. 2009: Does sea ice influence Greenland ice sheet surface-melt?, Environmental Research Letters, 4, 024 011.

Schölkopf, B. and Smola, A. 2002: Learning with Kernels, MIT press, Cambridge (MA).

Tedesco, M. 2007: A New Record in 2007 for Melting in Greenland, in: Eos, Transactions American Geophysical Union, vol. 88, p. 383.

Tedesco, M. and Miller, J. 2007: Observations and statistical analysis of combined active-passive microwave space-borne data and snow depth at large spatial scales, Remote Sensing of Environment, 111, 382–397.

P 19.2

Interactive multisensor change detection in remote sensing images via kernel canonical correlation transformation

Volpi Michele[1], Matasci Giona[1], Kanevski Mikhail[1], Tuia Devis[2]

[1] *Centre de Recherche en Environnement Terrestre (CRET), University of Lausanne, UNIL-Mouline, CH-1015 Lausanne. (michele.volpi@unil.ch)*
[2] *Laboratoire des Systèmes d'Information Geographique (LaSIG), École Polytechnique Fédérale de Lausanne, EPFL Station 18, CH-1015 Lausanne.*

Multisensor change detection is defined as the process of identifying changes in two (or more) images of the same geographical area acquired by different instruments at different time instants (Bruzzone and Fernandez-Prieto, 2000; Mercier et al., 2008; Longbotham et al., 2012). In this study, we investigate the feasibility of multisensor change detection in remote sensing images by interactively exploiting the user knowledge in the process. Recently, a system able to make two images acquired by different sensors comparable has been proposed (Volpi et al., 2013). Such a system allows to perform accurate pixelwise spectral change detection relying on the difference image. The process exploits a nonlinear transformation, the kernel canonical correlation analysis (kCCA) (Bach and Jordan, 2002), to reproject both the involved images in a common space in which unchanged pixels are maximally correlated and thus comparable, making their difference the closest possible to zero. After this statistical image alignment step, standard change detection methods may be applied to obtain the change map.

However, a major issue was the choice of the samples used to compute the kernel-based alignment, that is, selecting appropriate examples from which to compute the transformation. In this contribution, we study the possible synergy with the user in selecting such samples. The user is asked to iteratively select from the transformed difference image a subset of samples representing either unchanged pixels and unwanted changes (e.g. phenological differences). To drive the process, two measures are used to provide information about the quality of the alignment: the correlation of the transformed components implicitly provided by the kCCA, and the distance of the bi-temporal samples in the transformed space.

Finally, after the alignment step, the change vector analysis (CVA) is applied to perform change detection from the transformed difference image (Bruzzone and Fernandez-Prieto, 2000). Furthermore, the samples that have been iteratively selected by the user are included in the automatic process. Those pixels help the system to choose a proper threshold discriminating whether a change has occurred or not at a given pixel location.

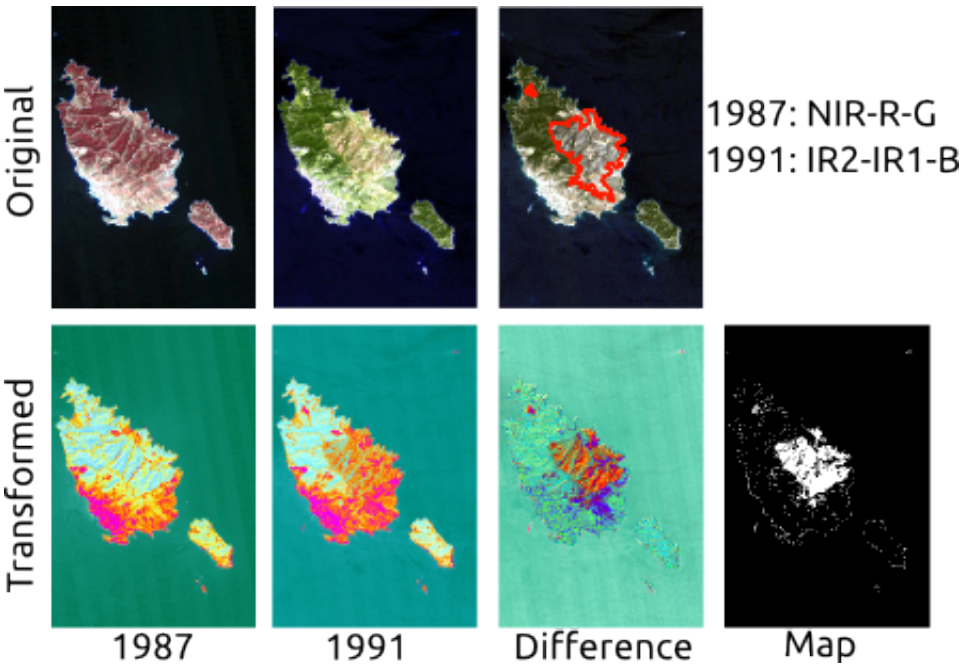

Figure 1: The multisensor change detection system. Original images (false colors) are aligned to obtain comparable, tranformed images of equal dimensionality enhancing changed area in their difference.

REFERENCES

F. R. Bach and M. I. Jordan, "Kernel independent component analysis," Journal of Machine Learning Research, vol. 3, pp. 1–48, 2002.

L. Bruzzone and D. Fernandez-Prieto, "Automatic analysis of the difference image for unsupervised change detection," IEEE Transactions on Geoscience and Remote Sensing, vol. 38, no. 3, pp. 1171–1182, 2000.

N. Longbotham, F. Pacifici, T. Glenn, A. Zare, M. Volpi, D. Tuia, E. Christophe, J. Michel, J. Inglada, J. Chanus-sot, and Q. Du, "Multi-modal change detection, application to the detection of flooded areas: Outcome of the 2009-2010 data fusion contest," IEEE Journal of Selected Topics on Applied Earth Observation, vol. 9, no. 6, pp. 331–342, 2012.

G. Mercier, G. Moser, and S. B. Serpico, "Conditional copulas for change detection in heterogeneous remote sensing images," IEEE Transactions on Geoscience and Remote Sensing, vol. 46, no. 5, pp. 1428–1441, 2008.

Volpi, M.; de Morsier, F.; Camps-Valls, G.; Kanevski, M. and Tuia, D., "Multi-sensor change detection based on nonlinear canonical correlations", *IEEE International Geosciences and Remote Sensing Symposium IGARSS 2013, Melbourne (AUS), 2013.*